[CANCER RESEARCH 64, ●●●–●●●, July 15, 2004]

Collagenase Increases the Transcapillary Pressure Gradient and Improves the Uptake and Distribution of Monoclonal Antibodies in Human Osteosarcoma Xenografts[1]

Live Eikenes,[1] Øyvind S. Bruland,[3] Christian Brekken,[2] and Catharina de Lange Davies[1]

[1]Department of Physics and [2]Department of Circulation and Medical Imaging, The Norwegian University of Science and Technology, Trondheim, Norway; and [3]Department of Radiotherapy and Oncology, The Norwegian Radium Hospital, Oslo, Norway

ABSTRACT

Cancer therapy based on tumor-selective macromolecules may fail due to the elevated interstitial fluid pressure (IFP) that reduces the transvascular and interstitial convection in solid tumors. Modulation of the tumor extracellular matrix (ECM) may reduce IFP and enhance transvascular filtration and interstitial transport of macromolecules. We therefore measured the effect of the ECM-degrading enzyme collagenase on IFP and microvascular pressure (MVP) in human osteosarcoma xenografts using the wick-in-needle and micropipette methods, respectively. The tumor uptake and distribution of an osteosarcoma-associated monoclonal antibody (TP-3) after i.v. injection of collagenase were analyzed using confocal laser scanning microscopy. Collagenase (0.1%) reduced both IFP (45%) and MVP (60%), but the kinetics of the recoveries differed, because MVP had recovered by the time IFP reached its minimum level. Thus, collagenase increased the transcapillary pressure gradient, inducing a 2-fold increase in the tumor uptake and improving the distribution of the monoclonal antibody, which was localized further into the tumor. To study the mechanism of the reduction in MVP, mean arterial blood pressure was measured and found not to be effected by the collagenase treatment. The reduction in MVP was rather due to reduced vascular resistance because microvascular-associated collagen was totally or partially disintegrated. Although collagenase may favor metastasis and thus not be clinical relevant, this study shows proof of principle that degradation of the ECM leads to a favorable change in the transvascular pressure gradient, thereby increasing antibody penetration and binding to tumor cells.

INTRODUCTION

Tumor-selective macromolecules such as monoclonal antibodies and DNA vectors for gene therapy generally show low uptake in solid tumors. A major obstacle to the successful delivery of large therapeutic molecules is the high interstitial fluid pressure (IFP), which reduces transvascular convection and generates an outward interstitial flux toward the periphery of the tumor (1). Thus, macromolecules are not delivered in sufficient quantities for the therapy to be successful. Both transvascular and interstitial transport are governed by convection and diffusion (2). For large therapeutic molecules, diffusion is extremely slow (3), and a high transcapillary pressure gradient is even more important.

Transvascular convection is mainly a result of the difference between microvascular and interstitial pressure. However, because the elevated IFP is driven by the high microvascular pressure (MVP), the transvascular pressure gradient in tumors is low (4). Interstitial convection is governed by IFP gradients and hydraulic conductivity, which depend on the interstitial space, composition, and structure of the tissue. The interstitium consists of a protein network embedded in a hydrophilic gel of glycosaminoglycans and proteoglycans. It is not clear, however, to which degree the network of fibrillar collagen or the glycosaminoglycan gel limits the transport of macromolecules. Interstitial hydraulic conductivity has been found to correlate inversely with collagen (5) and glycosaminoglycan content (5, 6), as well as with IFP (7). The interstitial diffusion coefficient also correlated inversely with collagen (8–10) but positively with hyaluronan content (9). The uptake of nonspecific IgG did not, however, correlate with the amount of extracellular matrix (ECM) constituents but correlated inversely with IFP (11). This may suggest that the structure of ECM rather than the amount of the ECM constituents is the most important factor for macromolecule uptake. Manipulating the collagen/glycosaminoglycan assembly or structure may therefore improve the transvascular and interstitial transport of macromolecules.

Various treatments have been used to modulate the tumor interstitium (12–14). We have previously reported that intratumoral injection of hyaluronidase, which degrades hyaluronan a major interstitial glycosaminoglycan, reduces IFP temporarily (12) and increases antibody uptake (15). In this present work, we therefore wanted to study whether the disintegration of the structural collagen network in the interstitium had a similar impact on IFP and antibody uptake as the disintegration of hyaluronan gel. To learn more about the mechanisms underlying the tumor uptake of macromolecules, IFP and MVP were measured in human osteosarcoma xenografts by the wick-in-needle and micropipette methods, respectively, after i.v. injection of collagenase. The effect of collagenase on the uptake and distribution of an osteosarcoma-associated monoclonal antibody (TP-3) was analyzed using confocal laser scanning microscopy. However, there may be concerns related to the clinical use of collagenase, because the enzyme is not tumor selective and facilitates the formation of metastases (16).

MATERIALS AND METHODS

Human Osteosarcoma Xenograft Models

Tumors were grown s.c. in the hind leg in 7–9-week-old female athymic BALB/c-*nu/nu* mice (Taconic; M&B, Ry, Denmark) by injecting a 100-μl suspension of 2×10^6 human osteosarcoma cells from the cell line OHS (17). Tumor width and length were measured with a digital caliper, and volumes were estimated using the prolate ellipsoid volume formula ($V = \pi/6 \times (\text{width})^2 \times \text{length}$). The xenografts were grown for 3–6 weeks, and tumor size varied from 0.35 to 0.60 cm^3. The animals were kept under pathogen-free conditions and allowed food and water *ad libitum*. All surgical and experimental procedures were performed under anesthesia using s.c. injection of Hypnorm:Dormicum:sterile water, 1:1:2; 1 ml/kg bodyweight (Janssen Pharmaceutical, Beerse, Belgium, and Alpharma AS, Oslo, Norway, respectively), and the mice were placed on a heating pad at 37°C.

IFP and MVP Measurements

Wick-in-Needle Technique. IFP was measured using the wick-in-needle technique (18). In brief, a hypodermic needle (size G23) was placed centrally in the tumor and connected to a pressure transducer (SensoNor 840, Horten, Norway) via polyethylene tubing filled with sterile heparinized PBS (70

Received 5/23/03; revised 4/2/04; accepted 5/6/04.

Grant support: Norwegian Cancer Society.

The costs of publication of this article were defrayed in part by the payment of page charges. This article must therefore be hereby marked *advertisement* in accordance with 18 U.S.C. Section 1734 solely to indicate this fact.

Requests for reprints: Catharina de Lange Davies, Department of Physics, The Norwegian University of Science and Technology, Høgskoleringen 5, 7491 Trondheim, Norway. Phone: (47) 735-93688; Fax: (47) 735-97710; E-mail: catharina.davies@phys.ntnu.no.

DOI: 10.1158/0008-5472.CAN-03-1472

units/ml). Pressures were monitored online using a MacLab analog-to-digital recording system with a sampling rate of 4 Hz (MacLab4/e; ADInstruments, Hastings, United Kingdom). Fluid communication between the needle and the tumor tissue was tested by compressing and decompressing the tubing, and it was accepted when the IFP did not vary by more than 20%.

After reaching a stable IFP value, 100 μl of collagenase (Clostridiopeptidase A; Sigma, St. Louis, MO) in PBS were injected into the tail vein. The IFP was recorded continuously up to 100 min after the injection, and after 2, 6, 7, and 24 h in a subgroup of animals. Control animals received 100 μl of PBS.

MP Technique. MVP and IFP gradients were measured using micropipettes and a servo-controlled counterpressure system (19). The counterpressure was generated to balance the change in the electrical resistance in the micropipette. The generated counterpressure represents the actual MVP or IFP and was amplified and recorded using the same MacLab analog-to-digital recording system used for the wick-in-needle technique. A micromanipulator (Narishige, Tokyo, Japan) and a stereomicroscope were used to maneuver the micropipette and measure the depth of insertion into the tumor. The micropipettes were made from borosilicate glass capillaries (1.0-mm outer diameter $\times$ 0.58-mm inner diameter) using a horizontal pipette puller (Narishige). A microbeveller (WPI, Hertfordshire, United Kingdom) grinded the tips of the micropipettes, resulting in a tip diameter of about 5 μm. The skin overlaying the tumor was removed before micropuncture, and zero pressure was recorded in the saline film covering the wound.

MVP was measured in one peripheral vessel per tumor. The microvessel had a diameter of approximately 50 μm, and the length of the vessel that was visible at the tumor periphery was at least 1 mm. After the initial MVP measurement, 100 μl of 0.1% collagenase in PBS were administrated i.v. The micropipette was withdrawn during the injection to prevent breakage. MVP was measured up to 100 min after the injection of collagenase but was not measured continuously. The pipette had to be replaced during the experiment because of frequent breakage and clogging. Control animals received 100 μl of PBS i.v.

Central IFP and peripheral MVP were measured simultaneously before collagenase injection in a subgroup of mice using the wick-in-needle and micropipette techniques, respectively.

Mean Arterial Blood Pressure (MABP) Measurements

MABP was measured using the carotid cannulation method as described elsewhere (12). In brief, the left carotid artery was isolated, and the cranial end of the artery was ligated. A metal clamp was applied caudally to stop the blood flow during cannulation. A polyethylene catheter filled with heparinized PBS was inserted through a hole cut proximally to the cranial ligature, and another suture was tied tightly around the tubing and artery. The clamp was removed, the end of the tubing was connected to a pressure transducer, and the pressure monitored online using a MacLab analog to digital converter, as described for the IFP measurements.

Antibodies

The murine monoclonal antibody TP-3 (IgG 2b) was developed in response to immunization of mice with human osteosarcoma cells and binds to a specific epitope on a M_r 80,000 monomeric polypeptide cell membrane antigen (20). The irrelevant murine monoclonal antibody UPC-10 (Flow, Inc., Rockville, MD) was used as a negative control.

AQ: A

TP-3 and UPC-10 were labeled with biotin in accordance with Bayer and Wilchek (21). In brief, biotin (Vector Laboratories, Burlingame, CA) dissolved in DMSO (5 mg/ml) was added in 10$\times$ molar excess to the antibodies in 0.5 M borate buffer (pH 8) and incubated on a horizontal rotational shaker at 4°C overnight. One M ethanolamine (pH 8) was added to bring the final solution to 0.1 M before incubation for 2 h at room temperature. Free biotin was removed by dialysis.

Biotinylated TP-3 (1.1 mg/ml in 200 μl) was administrated by tail vein injection 100 min after an i.v. injection of 0.1% collagenase. The same amounts of TP-3 or UPC-10 were also injected into mice 100 min after i.v. administration of PBS (200 μl). The mice were sacrificed by cervical dislocation 24 h later.

Immunofluorescence Staining

The tumors were excised, embedded in Tissue Tec (O.C.T.; Histolab Products, Gøteborg, Sweden), and frozen in liquid N_2; and 5-μm-thick tumor sections were mounted on slides. Before staining, the sections were fixed in acetone and incubated with 1% BSA in PBS to block nonspecific binding.

Blood vessels were labeled in a four-layer staining reaction: rat-antiCD31 (diluted 1:30; PharMingen, San Diego, CA) incubated for 1 h, rabbit-antirat-IgG (diluted 1:200; Dako Corp., Oslo, Norway) incubated for 30 min, goat-antirabbit-Dako Envision (100 μl; Dako Corp.) incubated for 30 min, and rabbit-antigoat-IgG-Alexa Fluor 488 (10 μg/ml; Molecular Probes, Eugene, OR) incubated for 30 min. The slides were incubated at room temperature in a humid chamber and rinsed with PBS after each incubation.

The biotinylated antibodies were stained using a tyramide signal amplification kit (NEN; Life Science Products, Boston, MA) and streptavidin-Alexa Fluor 546 (1:100; Molecular Probes) incubated for 30 min in a humid chamber at room temperature. The slides were rinsed with a buffer supplied in the amplification kit before and after each incubation and finally with distilled water to remove salt crystals.

Tissue interstitial collagen type I was colocalized with blood vessels in tumor sections from mice sacrificed 1 h after collagenase treatment. Collagen was labeled using goat-antihuman collagen type I (1:20; Biodesign, Kennebunk, ME) and streptavidin-Alexa Fluor 546 (1:100; Molecular Probes), with incubation periods of 60 and 45 min, respectively, in a humid chamber at room temperature. The slides were rinsed with PBS after each incubation.

Confocal Laser Scanning Microscopy

The uptake and distribution of antibodies and the localization of tumor vessels and interstitial collagen were studied using confocal laser scanning microscopy (LSM 510; Zeiss, Jena, Germany). Colocalization of TP-3 and blood vessels, as well as collagen and blood vessels, was done using a $\times$20/0.3 objective. The irrelevant antibody and blood vessels were studied using a $\times$40/1.2 water objective. The 488-nm argon and 543-nm HeNe lasers were used to excite Alexa Fluor 488 and Alexa Fluor 546, respectively.

The uptake of TP-3 was quantified by measuring average fluorescence intensity per image by calculating the sum of all pixel values (0–255 gray levels) divided by the number of pixels in the image. Autofluorescence from unstained sections was not detectable with the instrument settings used. The fluorescence intensity was measured along a horizontal and a vertical radial track from the periphery through the center of the section. This was done for six collagenase-treated and three control tumors, and 10 sections/tumor were analyzed. Five to 10 images were recorded along the track, depending on the diameter of the section. The distance between each section was 250 μm.

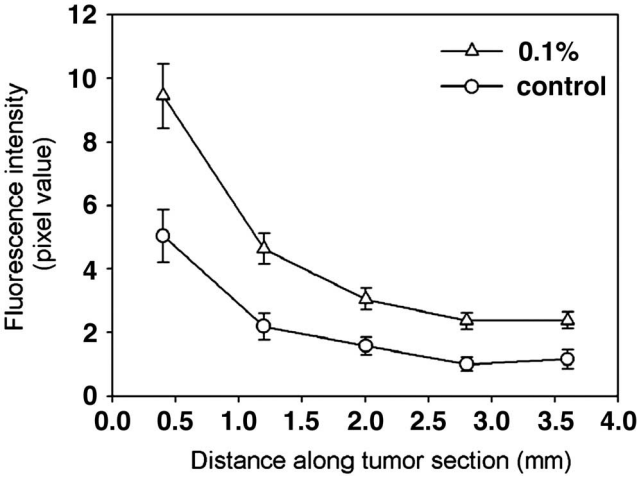

Fig. 1. Normalized interstitial pressure profiles $[P(r/R)/P_0]$ of five OHS s.c. tumors as a function of the normalized radial position (r/R). R is the tumor radius and r is the distance from the tumor periphery. Each symbol represents one tumor, and each point represents one measurement in the tumor. The *solid line* represents the steady-state solution of the IFP; $P(r/R)/P_0 = [1 - (\sinh(\alpha \cdot r/R)/(r/R \cdot \sinh(\alpha))]$ fitted for the hydraulic conductivity ratio $[\alpha^2 = R^2(L_p/K)(S/V)]$ $\alpha^2 = 380$ ($r = 0.9$, $P < 0.0001$; Ref. 22).

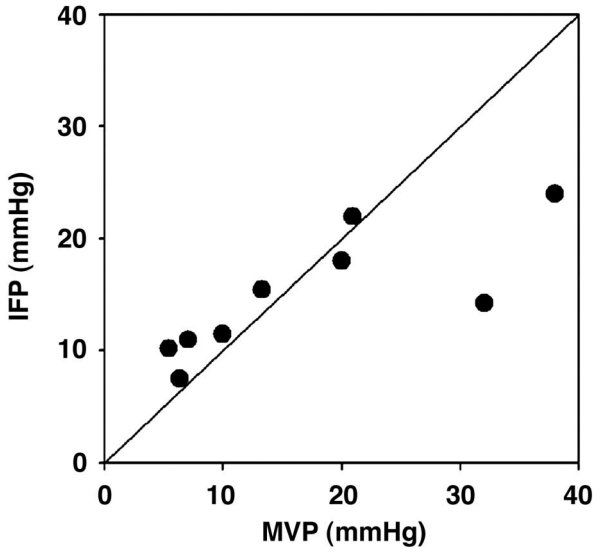

Fig. 2. Central IFP *versus* peripheral MVP in nine OHS s.c. tumors. The *solid line* represents MVP = IFP.

Statistical Analysis

The changes in pressure relative to pretreatment values were determined individually for each tumor and then averaged. Gaussian data were analyzed using Student's t tests. The nonparametric Wilcoxon's signed-rank test was used for data that were not Gaussian. All statistical analyses were performed using the significance criterion $P = 0.05$.

RESULTS

IFP and MVP. The IFP demonstrated a steep gradient in the periphery of the s.c. xenografts (0–0.4 mm into the tumor) and a high uniform pressure throughout the central part of the tumor (Fig. 1). The experimental data fit the steady-state solution of the equation describing IFP when modeling the tumor mathematically as a poroelastic medium (22).

Central IFP and peripheral MVP were measured simultaneously and found to correlate significantly ($R^2 = 0.63$, $P = 0.011$). The IFP and MVP were almost equal except in two tumors in which MVP was approximately twice IFP (Fig. 2). The overall mean showed no significant difference between IFP (14.9 ± 5.6 mmHg) and MVP (17.0 ± 11.7 mmHg). No correlation was found between the central IFP and the tumor volume (data not shown).

Effect of Collagenase on IFP. Collagenase induced a dose-dependent reduction in IFP (Fig. 3). Systemic administration of 0.1 and 0.01% collagenase reduced IFP by 45 and 26%, respectively. These maximum reductions were obtained approximately 100 and 60 min after the injections. The reductions differed significantly ($P < 0.01$), and both doses reduced IFP significantly compared with the controls ($P < 0.01$). The injection of PBS did not induce any significant reduction in IFP. Increasing the dose of collagenase to 0.5 and 1% was lethal.

The IFP reduction demonstrated a rapid initial drop (time constant τ_v), followed by a slower decay (time constant τ_i; Fig. 3*A*). The two time constants resulting from the best curve fit of a theoretical biexponential response to the average experimental response were $\tau_v \approx 300$ s and $\tau_i \approx 2500$ s for 0.01% collagenase and $\tau_v \approx 250$ s and $\tau_i \approx 5000$ s for 0.1% collagenase.

Intratumoral injection of collagenase showed a similar, but faster IFP response (data not shown). IFP was reduced by approximately 44 and 67% 60 min after the intratumoral injection of 0.1 and 0.5% collagenase, respectively.

The recovery of IFP was rather slow. IFP was measured at 2, 6, and 7 h after i.v. administration of 0.1% collagenase. During this time period, there was not a significant rise in IFP (Fig. 3*B*). After 24 h, IFP had returned to the initial level in mice given 0.01% collagenase, whereas 0.1% collagenase showed slower recovery as IFP had not completely reached its initial level (Fig. 3*B*).

Effect of Collagenase on MVP and MABP. Collagenase induced a rapid reduction in and recovery of MVP (Fig. 4). The maximum reduction in MVP was reached after approximately 40 min, and the MVP had recovered within 100 min after the administration of 0.1%

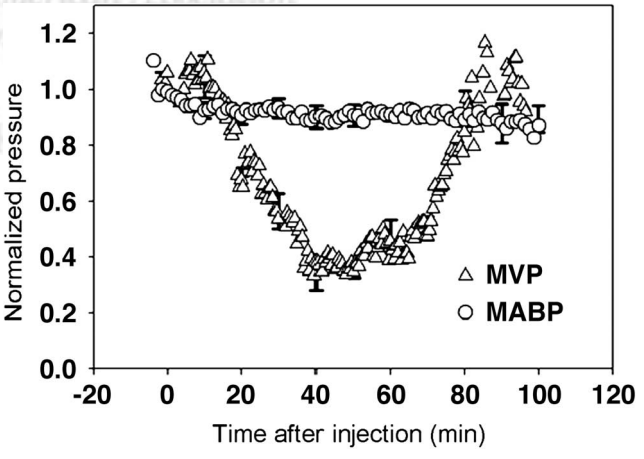

Fig. 4. Average MVP ($n = 2$–6; △) and MABP ($n = 4$; ○) response after i.v. injection of 0.1% collagenase. MVP was not measured continuously, and the data are based on different time intervals for $n = 10$ mice. Each time point is the average of two to six measurements. The *bars* indicate SE at some time points.

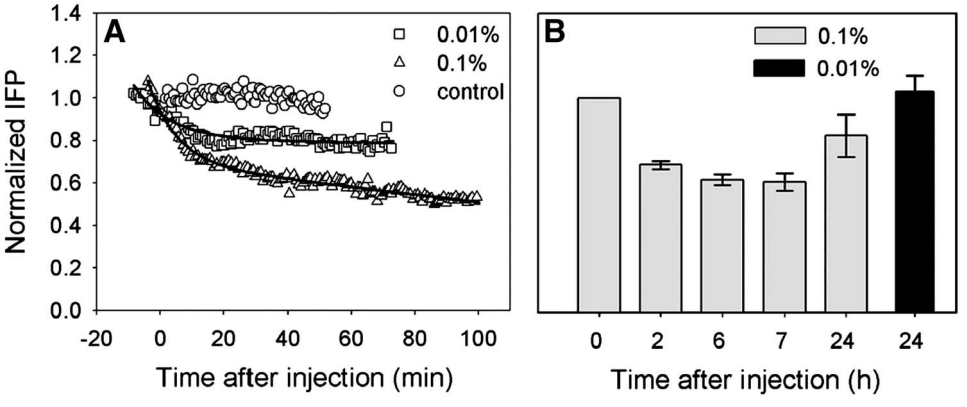

Fig. 3. *A,* representative IFP response as a function of time after i.v. injection of PBS (○), 0.01% collagenase (□), and 0.1% collagenase (△). IFP was normalized to the pressure before collagenase injection. The *solid lines* represent the theoretical curves, $IFP(t) = A_o\exp(-t/\tau_v) + B_o\exp(-t/\tau_i) + IFP(t = \infty)$ fitted by nonlinear regression to the experimental data. *B,* histogram representing the normalized IFP response after i.v. injection of 0.1% collagenase (*gray*) at $t = 0$, 2, 6, 7, and 24 h and 0.01% collagenase (*black*) at $t = 24$ h. The *bars* indicate SE.

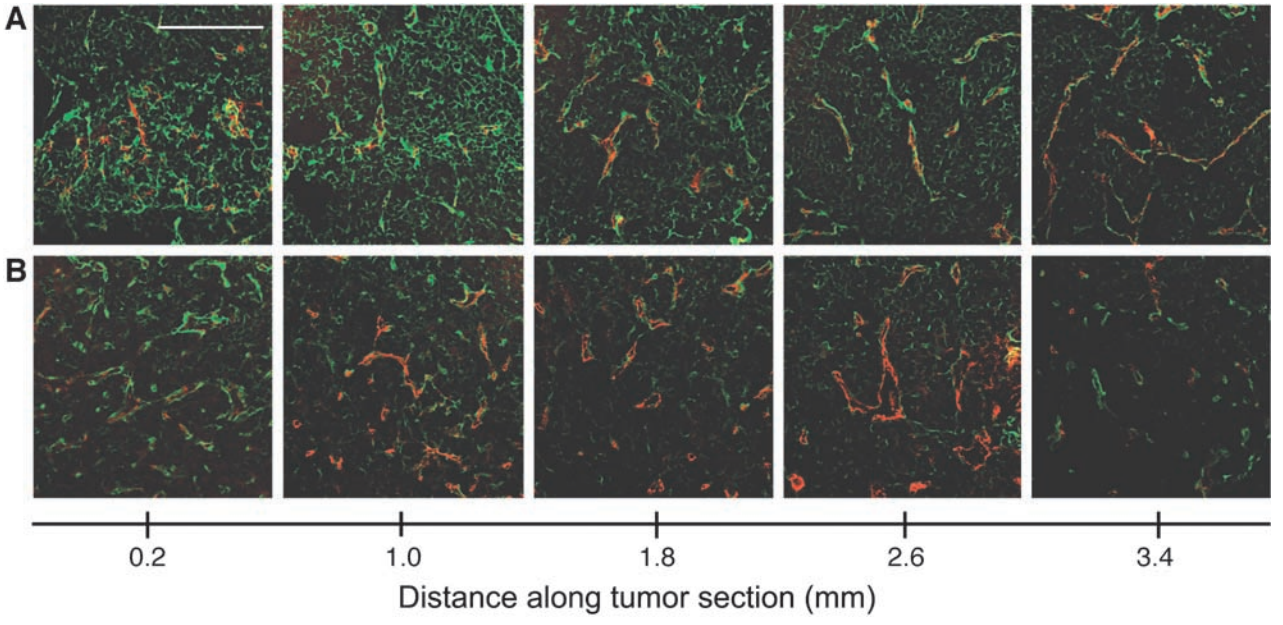

Fig. 5. Distribution of TP3 antibody (*green*) and blood vessels (*red*) in two representative tumors treated with 0.1% collagenase (*A*) and PBS (*B*). The sections were taken at a depth of approximately 4 mm from the surface of the tumor, and the five pictures were taken from the periphery to the center of the tumor. *Bar* = 50 μm.

collagenase. Collagenase did not induce any significant reduction in MABP.

Effect of Collagenase on Antibody Distribution. Collagenase improved the distribution of the monoclonal antibody TP-3 recognizing cell surface osteosarcoma-associated antigen. The distribution of the antibody was heterogeneous both in the treated and untreated F5 tumors, located mainly in the periphery of the tumors (Fig. 5). In collagenase-treated tumors, the antibody penetrated further into the tumors and was localized both in close proximity to and further away from blood vessels. Irrelevant antibody was, however, only located around endothelial cells throughout the whole tumor and did not F6 penetrate away from the vessels and into the interstitium (Fig. 6).

Effect of Collagenase on Antibody Uptake. To obtain quantitative data on antibody uptake, the fluorescence intensity of the antibody was quantified by estimating the mean pixel values per image F7 (Fig. 7). The data showed that the uptake of antibody was approximately four times higher in the periphery compared with the central part in both treated and untreated tumors. Collagenase increased the tumor-uptake of the antibody. A 2-fold (varying from 1.9–2.4) significant increase in antibody uptake was found in all parts of the collagenase-treated tumors compared with the controls. Antibody uptake was also measured as the fluorescence pixel area per image and found to be consistent with the pixel values (data not shown).

Effect of Collagenase on Tumor Tissue Collagen Type I. Immunofluorescence staining of collagen type I showed that collagenase degraded the collagen surrounding the tumor vessels (Fig. 8). In F8 untreated tumors, bundles of collagen type I were located heterogeneously throughout the tumor, and intense collagen staining was observed at the rim of the tumors. Nearly all of the blood vessels were surrounded by a layer of collagen type I, although it did not always cover the whole endothelial layer. In the collagenase-treated tumors, nearly all of the blood vessels had lost their collagen lining, either totally or partially, 1 h after the treatment, whereas collagen not closely associated with the vasculature appeared to be intact at that point in time.

DISCUSSION

Collagenase was found to increase the transcapillary pressure gradient temporarily, thereby improving the uptake and distribution of

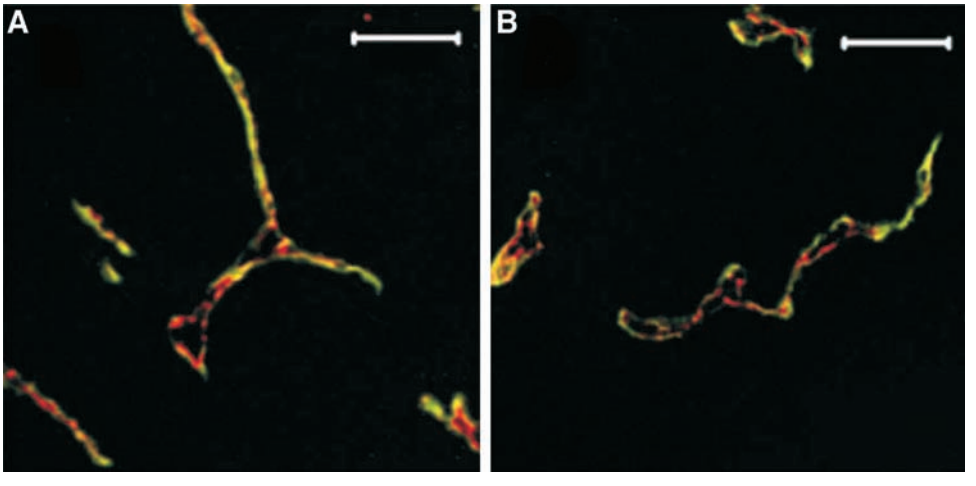

Fig. 6. Distribution of unspecific antibody (*green*) and blood vessels (*red*) in the periphery (*A*) and central part (*B*) of one representative tumor. The section is at a depth of approximately 3 mm from the surface of the tumor. *Bar* = 50 μm.

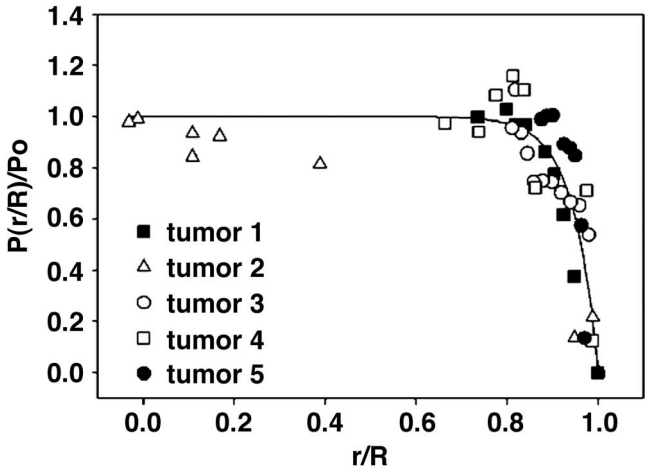

Fig. 7. Pixel value of fluorescent-labeled TP3 antibody after the injection of 0.1% collagenase ($n = 6$; △) and PBS ($n = 3$; ○), as a function of distance along the section. The results are the mean of six tumors and 10 sections/tumor. The images are taken along a vertical and horizontal track from the periphery to the center of the section. The *bars* indicate SE.

the monoclonal antibody TP-3 recognizing an osteosarcoma-associated antigen.

Induction of a Transcapillary Pressure Gradient. In untreated human osteosarcoma xenografts, the central IFP and peripheral MVP were both enhanced compared with normal tissue and appeared almost identical. The elevated central IFP demonstrated a steep peripheral gradient, as is also shown in tissue-isolated rat tumors (4). This consistency between different tumor models, as well as with mathematical modeling, indicates that the peripheral IFP gradient is a general phenomenon in tumors (7, 22).

Collagenase induced a reduction in both IFP and MVP, but the kinetics of recovery differed considerably. MVP recovered rapidly compared with IFP and had recovered completely by the time IFP reached its minimum level. The difference between the IFP and MVP recovery rates induces an increase in the transcapillary pressure gradient, lasting from 100 min to several hours after the administration of collagenase.

The decrease in MVP induced by collagenase may be explained by at least two different factors: the reduction in MABP and/or in the vascular resistance. Measurements of MABP demonstrated that the enzyme had no effect on MABP at the doses used here. The reduction in MVP is therefore probably due to a reduction in vascular resistance. This was confirmed by imaging the collagen type I network in the tumors. The interstitial collagen network was heterogeneous, with substantial amounts of collagen surrounding the microvessels. Microvessel-associated collagen has two important functions in the delivery of macromolecules: It influences the radii of the capillaries and the hydraulic conductivity of the vessel wall. Collagenase disintegrated the microvascular-associated collagen. This may increase the vessel radius, a major determinant of vascular resistance and associated with reductions in MVP and IFP (23). The degradation of microvascular-associated collagen may also increase vascular hydraulic conductivity, because collagenase has been reported to increase this hydraulic conductivity up to a factor of 10 (5).

The IFP reduction was characterized by a fast and a slow decay, described by two time constants, as also found after intratumoral injection of hyaluronidase (12). The time constants reflect transvascular and interstitial fluid exchange (22). The initial fast IFP reduction is therefore probably driven by the MVP reduction. The slower decay may be due to percolation of fluid through the interstitium and collagenase-induced degradation of the interstitium. Such degradation may increase hydraulic conductivity, thereby reducing IFP (7).

The difference in the recovery kinetics between MVP and IFP indicates that the two pressures recover by different mechanisms. The rapid recovery of MVP probably reflects an increase in vascular resistance. This may be due to changes in the viscoelastic properties of the tissue or synthesis of collagen by endothelial or other stromal cells in the proximity of blood vessels (24). The latter process, however, may be slower. The recovery of IFP, on the other hand, requires both transcapillary and interstitial filtration as well as remodeling of the interstitium. Interstitial collagen synthesis and the remodeling of the 3-dimentional ECM structure may be slow processes as reported in wound healing (25) and require more time than the increase in vascular resistance.

Implications for the Uptake of Therapeutic Macromolecules. The monoclonal antibody TP-3 bound specifically to the surface of osteosarcoma cells. This was demonstrated by the bright fluorescence surrounding tumor cells in xenografts treated with TP-3, and this fluorescence was not present in xenografts treated with the irrelevant antibody. Furthermore, the specificity of TP-3 has previously been confirmed by flow cytometry (26), and the administration of radiolabeled TP-3 or irrelevant UPC-10 antibody demonstrated approximately 20 times lower tumor:blood ratio for the irrelevant antibody, compared with TP-3 (15). Such a low tumor:blood ratio is consistent with the observed microdistribution of UPC-10 in the present work, because the antibody distribution was limited to endothelial cells.

The enhanced uptake of TP-3 in the tumor periphery correlated

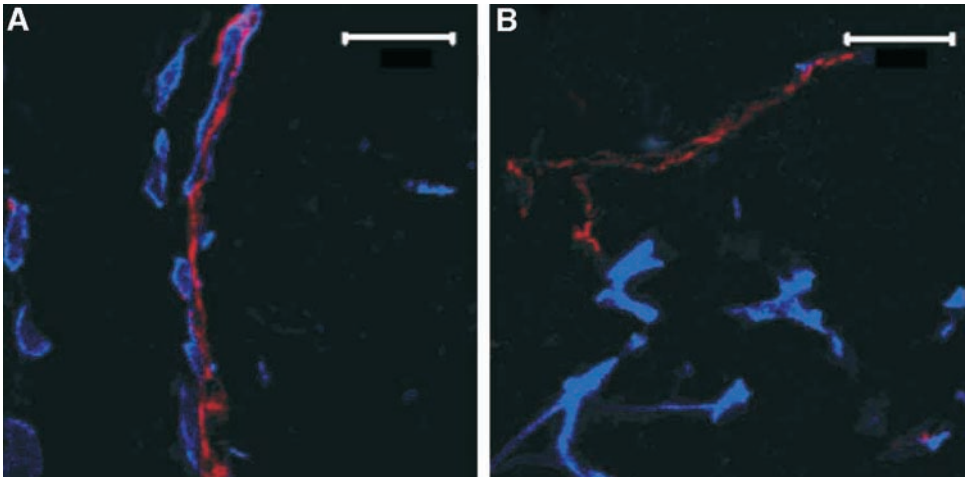

Fig. 8. Distribution of collagen (*blue*) and blood vessels (*red*) in two representative tumors treated with PBS (*A*) and 0.1% collagenase (*B*) 1 h after the injections. The sections were taken at a depth of approximately 3.5 mm from the surface of the tumor, and the images were taken from the central part of both sections. *Bar* = 200 μm.

spatially with the IFP gradient, where a transcapillary pressure gradient may favor peripheral antibody uptake. Hardly any antibody was located in the central part of the untreated tumor, where IFP was probably identical to MVP, thereby impeding convection. Collagenase increased the tumor uptake of TP-3 2-fold, and the antibody was located primarily around microvessels both in the tumor periphery and in the central parts. This is probably due to the induced transcapillary pressure gradient and increased vascular hydraulic conductivity caused by the degradation of vascular-associated collagen. Some TP-3 had penetrated away from the vessels due to increased interstitial hydraulic conductivity and/or increased diffusion coefficient, because collagenase is reported to increase these transport parameters (5, 8). Degradation of ECM may also increase the available interstitial volume (27), although damage of cells is reported to be more efficient than degradation of glycosaminoglycans in increasing the available volume fraction (28).

Various treatments and combinations of treatments appear to be successful in inducing a transcapillary pressure gradient and thereby increasing the uptake of therapeutic macromolecules. Periodic, repeated changes in IFP resulting from hyaluronidase (15) or angiotensin II (29) increased the uptake of monoclonal antibodies in xenografts. The repeated fluctuations in IFP probably induced a transcapillary gradient, although MVP was not measured in these studies; only MABP was measured. In the present work, however, both MVP and IFP were measured, thereby demonstrating a treatment-induced increase in the transcapillary pressure gradient and the dynamic of such a gradient.

By comparing the uptake of the osteosarcoma-associated antibody TP-3 after administration of collagenase with the uptake after hyaluronidase treatment found in a previous study (15), a higher antibody uptake after collagenase than after hyaluronidase treatment was found. In both studies doses of collagenase and hyaluronidase that reduced IFP to the same level were used. The low uptake of the irrelevant antibody UPC-10 was not enhanced by hyaluronidase (15). The comparison of collagenase and hyaluronidase thus shows that the degradation of the structural protein network is more efficient than the degradation of the hyaluronan gel, with respect to macromolecule uptake. Although hyaluronidase is reported to improve the therapeutic outcome of chemotherapy (30, 31), caution must be taken when using collagenase clinically as the enzyme may favor metastases (16, 32).

The present work demonstrates the importance of inducing a transcapillary pressure gradient for increasing the uptake and improving the distribution of therapeutic macromolecules in solid tumors. The induction of a transcapillary pressure gradient has important clinical implications, especially when using larger therapeutic molecules such as DNA vectors and liposomes to deliver drugs, because the transport of such therapeutic macromolecules is mainly driven by pressure gradients.

ACKNOWLEDGMENTS

We thank Anniken Paulsen (Department of Physics, the Norwegian University of Science and Technology) for growing cells *in vitro* and injecting them into mice and Kristin Bringedal (Department of Pathology, University Hospital of Trondheim) for preparing frozen-tissue sections.

REFERENCES

1. Boucher Y, Baxter LT, Jain RK. Interstitial pressure gradients in tissue-isolated and subcutaneous tumors: implications for therapy. Cancer Res 1990;50:4478–84.
2. Jain RK. Delivery of molecular medicine to solid tumors: lessons from in vivo imaging of gene expression and function. J Controlled Release 2001;74:7–25.
3. Pluen A, Netti PA, Jain RK, Berk DA. Diffusion of macromolecules in agarose gels: comparison of linear and globular configurations. Biophys J 1999;77:542–52.
4. Boucher Y, Jain RK. Microvascular pressure is the principal driving force for interstitial hypertension in solid tumors: implications for vascular collapse. Cancer Res 1992;52:5110–4.
5. Weinberg PD, Carney SL, Winlove CP, Parker KH. The contributions of glycosaminoglycans, collagen and other interstitial components to the hydraulic resistivity of porcine aortic wall. Connect Tissue Res 1997;36:297–308.
6. Swabb EA, Wei J, Gullino PM. Diffusion and convection in normal and neoplastic tissue. Cancer Res 1974;34:2814–22.
7. Jain RK, Baxter LT. Mechanisms of heterogeneous distribution of monoclonal antibodies and other macromolecules in tumors: significance of elevated interstitial pressure. Cancer Res 1988;48:7022–32.
8. Netti PA, Berk DA, Swartz MA, Grodzinsky AJ, Jain RK. Role of extracellular matrix assembly in interstitial transport in solid tumors. Cancer Res 2000;60:2497–503.
9. de Lange Davies C, Berk DA, Pluen A, Jain RK. Comparison of IgG diffusion and extracellular matrix composition in rhabdomyosarcomas grown in mice versus in vitro as spheroids reveals the role of host stromal cells. Br J Cancer 2002;86:1639–44.
10. Pluen A, Boucher Y, Ramanujan S, et al. Role of tumor-host interactions in interstitial diffusion of macromolecules: cranial vs. subcutaneous tumors. Proc Natl Acad Sci USA 2001;98:4628–33.
11. de Lange Davies C, Engeseter B, Haug I, Ormeberg IW, Halgunset J, Brekken C. Uptake of IgG in osteosarcoma correlates inversely with interstitial fluid pressure, but not with interstitial constituents. Br J Cancer 2001;85:1968–77.
12. Brekken C, Bruland ØS, de Lange Davies C. Interstitial fluid pressure in human osteosarcoma xenografts: significance of implantation site and the response to intratumoral injection of hyaluronidase. Anticancer Res 2000;20:3503–12.
13. Pietras K, Östman A, Sjöquist M, et al. Inhibition of platelet-derived growth factor receptors reduces interstitial hypertension and increases transcapillary transport in tumors. Cancer Res 2001;61:2929–34.
14. Zlotecki RA, Boucher Y, Lee I, Baxter LT, Jain RK. Effect of angiotensin II induced hypertension on tumor blood flow and interstitial fluid pressure. Cancer Res 1993;53:2466–8.
15. Brekken C, Hjelstuen MH, Bruland ØS, de Lange Davies C. Hyaluronidase-induced periodic modulation of the interstitial fluid pressure increases selective antibody uptake in human osteosarcoma xenografts. Anticancer Res 2000;20:3513–20.
16. Curran S, Murray GI. Matrix metalloproteinases in tumour invasion and metastasis. J Pathol 1999;189:300–8.
17. Fodstad Ø, Brøgger A, Bruland Ø, Solheim ØP, Nesland JM, Pihl A. Characteristics of a cell line established from a patient with multiple osteosarcoma, appearing 13 years after treatment for bilateral retinoblastoma. Int J Cancer 1986;38:33–40.
18. Fadnes HO, Reed RK, Aukland K. Interstitial fluid pressure in rats measured with a modified wick technique. Microvasc Res 1977;14:27–36.
19. Wiederhielm CA, Woodbury JW, Kirk S, Rushmer RF. Pulsatile pressures in the microcirculation of frog's mesentery. Am J Physiol 1964;207:173–6.
20. Bruland Ø, Fodstad Ø, Stenwig E, Pihl A. Expression and characteristics of a novel human osteosarcoma-associated cell surface antigen. Cancer Res 1988;48:5302–9.
21. Bayer EA, Wilchek M. Protein biotinylation. Methods Enzymol 1990;184:159.
22. Netti PA, Baxter LT, Boucher Y, Skalak R, Jain RK. Time-dependent behavior of interstitial fluid pressure in solid tumors: implications for drug delivery. Cancer Res 1995;55:5451–8.
23. Griffon-Etienne G, Boucher Y, Brekken C, Suit HD, Jain RK. Taxane-induced apoptosis decompresses blood vessels and lowers interstitial fluid pressure in solid tumors: clinical implications. Cancer Res 1999;59:3776–82.
24. Du WD, Zhang YE, Zhai WR, Zhou XM. Dynamic changes of type I, III and IV collagen synthesis and distribution of collagen-producing cells in carbon tetrachloride-induced rat liver fibrosis. World J Gastroenterol 1999;5:403.
25. Betz P, Nerlich A, Wilske J, Tubel J, Penning R. Immunohistochemical localization of collagen types I and VI in human skin wounds. Int J Leg Med 1993;106:34.
26. Hjelstuen MH, Rasch-Halvorsen K, Bruland Ø, de Lange Davies C. Uptake, penetration, and binding of monoclonal antibodies with increasing affinity in human osteosarcoma multicell spheroids. Anticancer Res 1998;18:3153–62.
27. Krol A, Maresca J, Dewhirst MW, Yuan F. Available volume fraction of macromolecules in the extravascular space of a fibrosarcoma: implications for drug delivery. Cancer Res 1999;59:4136–41.
28. Krol A, Dewhirst MW, Yuan F. Effects of cell damage and glycosaminoglycan degradation on available extravascular space of different dextrans in a rat fibrosarcoma. Int J Hyperthermia 2003;19:154–64.
29. Netti PA, Hamberg LM, Babich JW, et al. Enhancement of fluid filtration across tumor vessels: implication for delivery of macromolecules. Proc Natl Acad Sci USA 1999;96:3137–42.
30. Baumgartner G, Fortelny A, Zänker KS, Kroczek R. Phase I study in chemoresistant loco-regional malignant disease with hyaluronidase. Reg Cancer Treat 1988;1:55–8.
31. Smith KJ, Skelton HG, Turiansky G, Wagner KF. Hyaluronidase enhances the therapeutic effect of vinblastine in intralesional treatment of Kaposi's sarcoma. J Am Acad Dermatol 1997;36:239–42.
32. Stamenkovic I. Extracellular matrix remodelling: the role of matrix metalloproteinases. J Pathol 2003;200:448–64.